

A viscosity-mediated model for relating the gloss and film thickness of coatings

Julio Uribe-Padilla (*)^{a,b,♣}; Moises Graells-Sobre^b; Juan Salgado-Valle^a; Julia López^a

^a-Chemical Engineering Department, Universitat Politècnica de Catalunya (UPC), EEBE, 08019, Av. Eduard Maristany 10-14, Barcelona, Spain.

^b-Polyurethane R & D Department, BASF Española S.L., Curtex Division, 08907, Carretera del Mig, 219, Barcelona, Spain.

[♣]- Currently at Production Department, Sumitomo Bakelite Europe Barcelona (SBHPP), SBEB, 08170, Gran Vial 4, Barcelona, Spain.

Highlights

- *Film thickness and gloss have been correlated for several glossy and matt coatings up to moderately thick layers.*
- *The model contemplates the hindering of film formation due to non-Newtonian behaviour as well as the presence and concentration of matting agents.*
- *A characteristic film-formation related time has been correlated to the levelling time.*
- *On this basis, a viscosity-film thickness relationship has been developed and validated.*

Abstract

Film thickness determines many key coating properties including gloss. Current literature hardly addresses the development of methods to directly correlate film thickness with gloss. Thus, the lack of accurate models hinders further product design and optimisation of coating products and processes. In this contribution, a previously derived gloss-viscosity relationship is turned into a gloss-film thickness mathematical model. Experimental results of both matting and glossy agents are found to be successfully predicted by a model that is revealed as a simple and useful tool for day-to-day calculations.

Keywords: Film thickness, gloss, matt, optical properties, coatings, mathematical modeling

Notation

1 1-Introduction

2 It has been recently reported that the gloss of a thickened-to-application hybrid
3 polyurethane dispersion (PUD) with matting purposes can be correlated with viscosity
4 [1]. These studies fostered revisiting the influence of other coating-relevant variables on
5 gloss [2], [3]. Special interest is now paid to film-thickness (FT or δ) and how it affects
6 optical properties and, in particular, matting efficiency. All coating manufacturers are
7 aware of the fact that FT is a key parameter not only from an aesthetic but also from a
8 practical point of view. For instance, the total cost (operational + raw materials) per unit
9 area of a coating process (C_c) is directly proportional to FT (i.e. $C_c \propto \frac{\bar{\delta} \cdot \rho}{Y_t \cdot w}$) being $\bar{\delta} \cdot \rho =$
10 Γ_c the total coating amount per unit area and $Y_t \cdot w$ the total transference yield per
11 solid content [4]. Furthermore, recent advances in coating studies have shown that FT
12 is also of paramount importance in electrical [5], [6], thermal [7], [8], mechanical [9]–
13 [11] or barrier properties [12]–[14].

14 Current chemical engineering trends ask for practical predictive models supporting
15 decision-making procedures and enhancing current and future product and process
16 design [15]–[17]. Past academic research concerning coatings' industry is based in
17 complex momentum balance problem formulations. Such approaches are
18 computationally expensive and require a deep understanding of transport-phenomena,
19 solving the Navier-Stokes equations for non-Newtonian fluids while taking into account
20 thermal effects and chemical reactions [18]–[27]. When tackling the optical properties
21 of coatings a similar situation is faced and intricate physics (like photonics, nonlinear
22 optics, etc.) must be dealt with [28]–[30]. Thus, an affordable approach combining film

23 thickness and gloss would be desirable for practical day-to-day calculations and
24 decision-making.

25 Therefore, the aims and contributions of this work are to:

- 26 • Derive a simple mathematical model that relates gloss and film thickness.
- 27 • Assess its usefulness and validity-limitations specially focusing on testing
28 different coatings and verifying functional dependences.

29 2-Modeling approach

30 2.1-Hypothesis

31 Let the following assumptions hold:

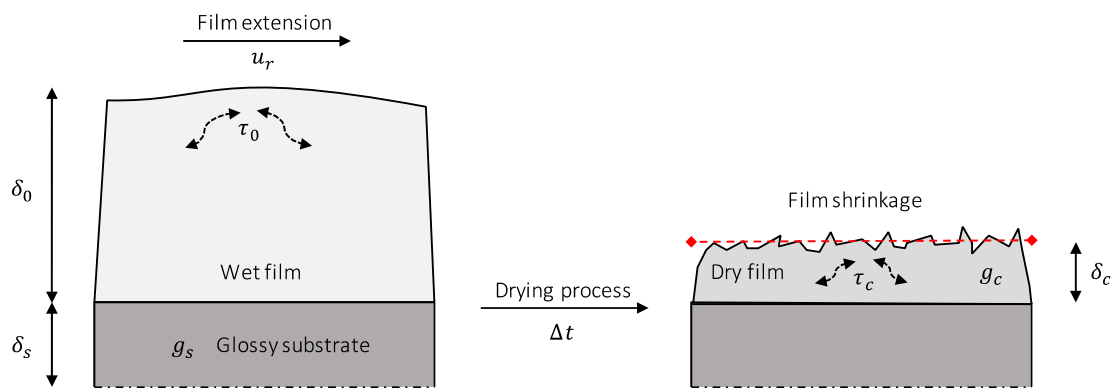
- 32 • The coating is well-represented by a prismatic geometry with its volume being
33 proportional to δ^3 .
- 34 • The application system is a roller blade-conveyor belt-like system.
- 35 • The relation between viscosity and FT can be conveniently represented by some
36 power law.
- 37 • FT is the most relevant dimension of the coating under study (i.e. final effects
38 are neglected [4]).
- 39 • Hiding-power related effects are only relevant below a minimum FT.
- 40 • The process is isothermal and no chemical interaction occurs between the
41 coating and the substrate nor the atmosphere.
- 42 • The system shows anisotropic behaviour.
- 43 • The liquid coating is or behaves like a Newtonian fluid for a sufficiently wide
44 shear rate interval.

- 45 • Average film thickness accounts for roughness and other surface texture
- 46 properties.
- 47 • No micro-sagging or micro-bubbling occurs.

48 2.2-Mathematical model

49 The problem addressed in this paper deals with how FT affects the final gloss of a given
 50 coating. If a suitable substrate (with gloss g_s) is to be coated up to a matting degree of
 51 g_c , it is desirable that $g_c \ll g_s$. The evolution of a liquid coated film when readily
 52 applied on such substrate and left to dry a certain amount of time Δt is illustrated in

53 Fig.1:



54 **Fig 1:** Film formation dynamics involved in the drying of a liquid film

55 Along the drying process, the mass of the film (m) and the associated matting content¹
 56 (w) need to satisfy the mass balance:

$$m_0 w_0 = m_f w_f \quad (1)$$

57 When all the solvent is evaporated $w_f = 1$, $m_f = m_0 w_0$ and a thinner coat is obtained.

58 Assuming a prismatic geometry the total volume of the film (V) is the product of film
 59 surface (S) and FT:

¹ More specifically $w = w_{Polymer} + w_{MA}$ or $w = \xi w_{MA}$ where $\xi = \frac{w_{Polymer}}{w_{MA}} - 1$. This specification is relevant when model parameters are to be correlated specifically with matting agent concentration.

$$V = S\delta \quad (2)$$

61 A real film will not have a perfectly smooth surface (Fig.2) because FT is generally
 62 inhomogeneous and varies both with length (x direction) and width (y direction). Hence
 63 surficial area must be calculated from roughness data from height (z direction) [31]:

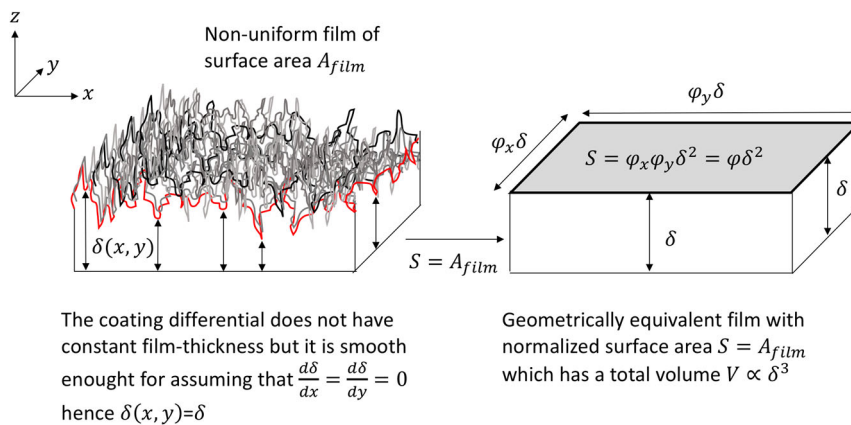
$$S = \iint_{film} \delta(x,y) dx dy \quad (3)$$

64 Since we are studying the effect of FT all geometric expressions should depend solely on
 65 a constant and representative value of FT. In Eq.4 all geometric complexity (film
 66 inhomogeneity, curvatures and waviness) is modelled by a lumped parameter φ that is
 67 obtained after evaluating the integral all over the film.

$$S = \left(\delta \int_0^{length} \Phi_x(x) dx \right) \cdot \left(\delta \int_0^{width} \Phi_y(y) dy \right) = \varphi_x \varphi_y \delta^2 = \varphi \delta^2 \quad (4)$$

68 Combining Eq.2 with Eq.4 it can be seen that the volume of the film is proportional to
 69 δ^3 .

$$V = S\delta = \varphi \delta^3 \quad (5)$$



70

71 **Fig 2:** Mathematical modeling of the film's surface in which a real film is transformed

72 in an equivalent smooth-surface film with identical surface.

73 Plugging Eq.5 in the mass balance (applying the definition of density) it is possible to

74 compute the following density ratio:

$$\frac{\rho_0}{\rho_f} = A_T \left(\frac{\delta_f}{\delta_0} \right)^3 \quad (6)$$

75 Eq.6 is useful given the difficulties in measuring near-to-solid coating bulk properties

76 [32]. A_T is a weight-fraction modified normalizing factor defined as:

$$A_T = \frac{\varphi_f w_f}{\varphi_0 w_0} \quad (7)$$

77 Several authors [33]–[38] have proposed film thickness-viscosity relationships (FTVRs)

78 that should follow a power-like model:

$$\mu \propto \delta^n \quad (8)$$

79 Nonetheless, intense debate is still found nowadays regarding n 's value. In general, n

80 can be found to fall between 1.43-1.50 (closer to theoretical predictions mostly based

81 on Landau-Levich theory [39], [40]) and 2.00 (verifying most empirical observations and

82 simpler modeling strategies [41]). A remarkable exception is that of asphalts [42],

83 cements [43] and bituminous substances [44] for which n can be either positive or

84 negative meaning that viscosity can decrease or increase with FT^2 .

85 Since this work is aimed at developing a practical tool FTVR will be used with $n = 2$. The

86 simplest model for which $\mu \propto \delta^2$ is derived from a force balance where capillary forces

87 match viscous forces. Despite this, an alternative reasoning (Eq.9 to Eq.15) based on

88 film-forming dynamics is proposed here, giving a new FTVR with $n = 2$.

89 During film formation, both surficial and internal stresses will appear due to a myriad of

90 causes [45], [46]. These momentum transports (Fig. 1) can experience transitions that

91 are here modelled by a characteristic periods λ^* [47], [48]. Letting ℓ be a characteristic

² The value of n is also highly technology-dependent being the $1.43 \leq n \leq 2$ values found in conveyor-belt like systems. Conversely wide range of processes carried out in continuous spinning disk reactors (SPR's) follow FTVRs with $2.8 < n < 3.2$. The effect of solvents also conditions final FT in drying films [72].

92 dimension of the system it is possible to correlate it with λ^* by means of viscosity and
 93 density. Furthermore if $\ell = \delta$ then:

$$\lambda^* = \frac{\rho \ell^2}{\mu} \rightarrow \lambda^* = \frac{\rho \delta^2}{\mu} \quad (9)$$

94 Along the film formation process several characteristic times can be of interest. The
 95 model focuses on the initial and final states represented in the mass balance (λ_0^* and λ_f^* ,
 96 respectively), which are here considered proportional:

$$\lambda_0^* = \alpha \lambda_f^* \quad (10)$$

97 where $0 < \alpha < 1$. Developing Eq.10 and introducing the definition of λ yields :

$$\frac{\rho_0}{\rho_f} = \alpha \left(\frac{\mu_0}{\mu_f} \right) \left(\frac{\delta_f}{\delta_0} \right)^2 \quad (11)$$

98 Rearranging Eq.11 a quadratic expression is obtained:

$$\mu_f = \alpha' \delta_f^2 \quad (12)$$

99 Where α' is:

$$\alpha' = \alpha \frac{\mu_0 \rho_f}{\delta_0^2 \rho_0} \quad (13)$$

100 It can be shown that α' includes time-related information giving higher credit to the
 101 modelling approach. In particular, the levelling time λ_{lev} (Eq.14) is invoked at this point
 102 as defined from Orchard's theory [49]–[51]. λ_{lev} is directly proportional to viscosity and
 103 inversely proportional to surface tension :

$$\lambda_{lev} \propto \frac{\mu}{\sigma} \quad (14)$$

104 From Eq.14 two conclusions can be drawn:

- 105 • The more viscous the coating the more time it takes for its film to flatten, hence
 106 remaining thicker.

107 • The lower the interfacial tension the more it takes the film to become smoother³.

108 The proportionality factor between λ_{lev} and $\frac{\mu}{\sigma}$ can be taken as an equivalent average

109 film thickness ($\bar{\delta}$)⁴. Considering also the Ohnesorge number ($Oh = \frac{\mu}{\sqrt{\rho\sigma\bar{\delta}}}$) the

110 proportionality factor can now be defined as a function of λ_{lev} :

$$\frac{\mu}{\bar{\delta}^2} = \frac{\rho}{\lambda_{Lev}} Oh^2 \rightarrow \alpha' = \frac{\rho}{\lambda_{Lev}} Oh^2 \quad (15)$$

111 Further mathematical treatment of the first part of Eq. 15 gives an interesting

112 nondimensional expression (Eq. 16):

$$113 \sqrt{\frac{Ca}{Bo}} = Oh \quad (16)$$

114 where Ca and Bo respectively stand for the Capillarity [54] and Bond numbers. Such

115 equation defines a working space [55] which characterizes the coating process⁵.

116 Finally, combining Eq.6 with Eq.11 and invoking the definition of $R = \frac{\mu_0}{\mu_f}$ leads to:

$$R = \frac{1}{\alpha} A_T \left(\frac{\delta_f}{\delta_0} \right) \quad (16)$$

117 This definition of R allows connecting both gloss and FT by means of viscosity. Providing

118 that DFT is significantly larger than average particle size, it seems intuitive to state that

119 the thicker the film the glossier it will be⁶. Choosing a previously derived model for

120 traditional silica-based MA [1]:

$$g = g_0 R^t \quad (17)$$

121 and combining it with Eq.16 a gloss-film thickness relationship (GFTR) is obtained.

³ This might seem counterintuitive since surface tension is a measure of the degree of substrate-coating affinity but this particular issue is thoroughly covered in literature .

⁴ The proportionality factor between λ_{lev} and $\frac{\mu}{\sigma}$ is $\frac{3f_z^4}{(2\pi)^4 h^3}$ and has equivalent length dimensions . It includes the ratio between film's striation degree (f_z) and a film thickness that includes roughness (h) [52]-[53]. Taking into account this, $\frac{3f_z^4}{(2\pi)^4 h^3} = \bar{\delta}$.

⁵ Further considerations about this result would be worth noting but are out of the scope of the present paper.

⁶ A thicker layer will mask substrate's effects and defects, yielding a smoother surface and hence, a glossier one. This is also in good agreement with leveling time since coatings with higher viscosity are glossier [1].

$$g = \mathcal{B}\delta_f^t \quad (18)$$

122 In which \mathcal{B} . Can be defined as:

$$\mathcal{B} = g_0 \left(\frac{A_T}{\alpha\delta_0} \right)^t \quad (19)$$

123 This expression confirms the general behaviour expected (gloss increases with FT).

124 Despite this, two questions arise concerning the case where no MA is applied at all and

125 if it adequately represents what happens for increasingly thicker layers. Regarding the

126 first one, a condition for the no-coating border (NCBC) must be defined:

$$\delta_f = 0 \rightarrow g = g_s \quad (20)$$

127 When no coating is applied, the recorded gloss must be that of the substrate. Once a

128 layer of product starts to deposit onto the substrate , the gloss readings start to change.

129 For thicknesses near or below average particle size, the coating's hiding power is

130 impoverished. Then, since no good substrate coverage is obtained, the matting

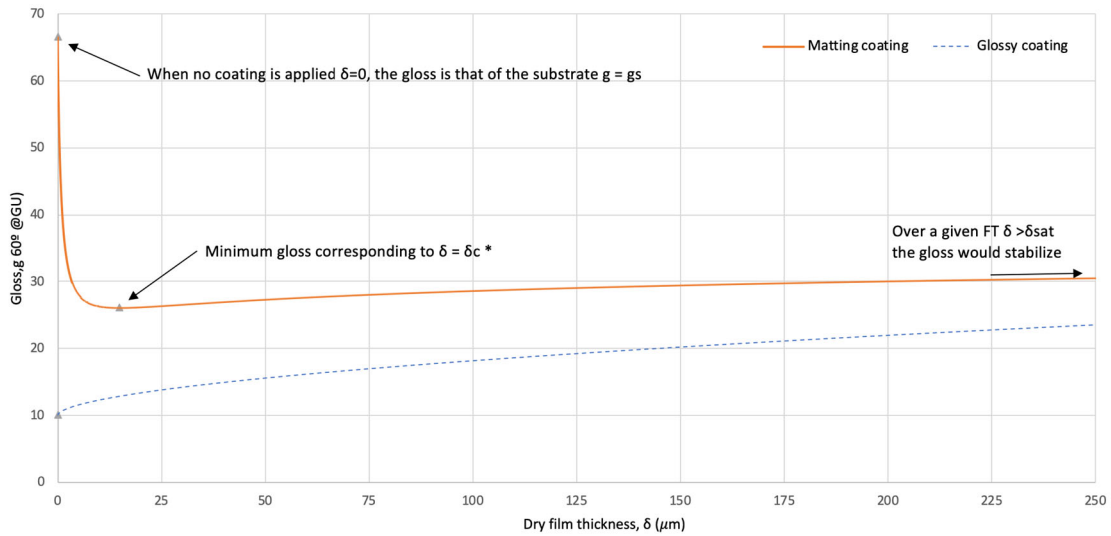
131 efficiency will be substantially lowered until a minimum film thickness is attained. Such

132 statement is in good agreement with early findings [56] . Going beyond the so-called

133 "optimum ⁷ " film thickness (δ_c^*) which leads to minimum gloss [57] spurs some

⁷ The optimum label is misleading though and, far from being a desirable situation, only consists of the minimum FT required for ensuring sufficient coverage [58] but without satisfying other requirements or design constraints. For instance, haptics and other surface texture indicators [59] are often not met when $\delta = \delta_c^*$.

134 considerations regarding thicker coatings.



135

136 **Fig. 3:** Qualitative graph showing a sample for a matting and a glossy coating up to $\delta \leq$
 137 δ_{sat} . The grey triangles show specific data points of interest.

138 The work of Fletcher [60] introduced two effectiveness factors respectively related to
 139 gloss (g_{eff}) and viscosity (μ_{eff}). Both parameters were involved in the derivation of
 140 two complementary gloss-concentration and viscosity-concentration models.

141 Whilst (for the traditional MA) μ_{eff} can be related to the intrinsic viscosity according
 142 the Krieger-Dougherty's theory [61], g_{eff} lacks of physical meaning. Further
 143 experimentation for various MAs at different concentrations showed that g_{eff}
 144 decreased with FT ($\delta > 20\mu m$) but a general trend could not be devised.

145 In the previous derivation for the same MA [1], g_{eff} and μ_{eff} were correspondingly
 146 rearranged as $g_{eff} = \ln(t_1)$ and $\mu_{eff} = 1/t_2$. Now, using the gloss-rheology model for
 147 the hybrid MA and recalling the expression of R found in Eq.16, Eq.21 is obtained:

$$\frac{g}{g_0} = 1 + t_1(\rho\delta^{t_2} - 1) \quad (21)$$

148 where $\wp = \left(\frac{A_T}{\alpha\delta_0}\right)^{t_2}$. Note that \wp is expected to be $\mathcal{O}_\wp(10^{-1})$ since average R was
 149 $\mathcal{O}_\wp(10^{-3})$. Moreover, g_{eff} is affected by FT [60] and consequently t_1 will change
 150 somehow with FT as well. Rearranging Eq.21, two different parts can be identified:

$$g = \underbrace{g_0(1 - t_1)}_{Part A} + \underbrace{t_1 g_0 \wp \delta^{t_2}}_{Part B} \quad (22)$$

151 For a given FT the gloss of the coating will be affected by-hiding power (Part A) or
 152 unaffected by it (Part B). This is reasonable taking into account Fig.3 and also with
 153 previous finding of the role of t_1 in maximum attainable gloss depletion [1].

154 Gloss can be directly related to the fraction of reflected light (reflectivity, r) [62], which
 155 in turn is related to some scattering coefficient (P_Ψ^∞) able of effectively promoting
 156 matting properties. Though the work of Fletcher [60] did not correlated g_{eff} with P_Ψ^∞
 157 or r it indeed indicated that g_{eff} depended on a diffuse response to illumination.
 158 Furthermore, assuming t_2 remains constant, t_1 is likely of being more sensitive to FT
 159 when $FT < \delta_c^*$, while gradually becoming less influenced by FT when $FT \geq \delta_c^*$ [63]. Hence,
 160 a reasonable hypothesis is that t_1 could be modeled as a (hyperbolic) trigonometric
 161 function.

$$t_1 = f_1(g_{eff}) = f_2(P_\Psi^\infty) = f_3(r) = \begin{pmatrix} \tanh \\ \coth^{-1} \\ \dots \end{pmatrix}(\delta) \quad (23)$$

162 This hypothesis is consistent with the Kubelka-Munk theory of reflectance and will be
 163 discussed later in the corresponding section. Until then, this unknown function of FT will
 164 be denoted as $J(\delta)$. In order to validate this last reasoning (Eq. 13) t_1 is now set
 165 constant. Then, differentiating Eq.12 and further integrating using the NCBC, Eq. 24 is
 166 obtained:

$$g = g_s + t_1 \rho \delta^{t_2} \quad (24)$$

167 Note now that Eq.24 represents the expected behaviour of a high-gloss coating applied
 168 to a substrate of gloss g_s as previously reported [65]. The fact that scattering coefficient
 169 does not depend on FT (*i. e.* $\frac{\partial t_1}{\partial \delta} = 0$) was already established for glossy substances
 170 such as white alkyds, glossy latexes and glossy paints [66].
 171 Additionally, recalling that $1.43 \leq n \leq 2$ it is expectable that $0.50 \leq t_2 \leq 0.70$ since
 172 they are inversely proportional. Then, t_1 can be expressed in different ways depending
 173 on the kind of coating under consideration.

$$t_1 = f_1(g_{eff}) = f_2(P_\Psi) = \begin{cases} \text{Glossy} & \frac{\partial t_1}{\partial \delta} = 0 \\ \text{Matt} & J(\delta) \end{cases} \quad (25)$$

174 In conclusion:

$$\begin{array}{l} \text{Glossy} \quad \frac{g}{g_0} = 1 + t_1(\rho \delta^{t_2} - 1) \\ \text{Matt} \quad \frac{g}{g_0} = 1 + J(\delta)(\rho \delta^{t_2} - 1) \end{array} \quad (26)$$

175

176 3-Experimental material and methods

177 This study has analysed experimental data from the literature and from freshly
 178 produced PUDs samples obtained from BASF's production site in L'Hospitalet de
 179 Llobregat in Catalonia (Spain). The samples from BASF were used as received.

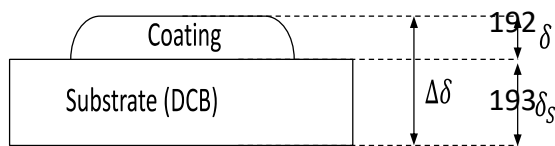
180 3.1-Polymer coatings

181 6-10 g of liquid sample where transferred via syringe to a standardized drawdown
 182 cardboard (WP-1, LENETA, New Jersey-United States). The card was secured to an
 183 application support bed. Several helical bar manual coaters from 10 to 100 μm of wet
 184 FT (NEUTREK, Eibar-Spain) where used for preparing the polymer films at an extension

185 speed of approximately 42 mm·s⁻¹. The polymer film was then dried on a clean and flat
 186 glass plate in a preheated air laboratory oven (ED115, Binder GmbH, Bohemia-Germany)
 187 keeping it at 60°C during 10 minutes. After being taken out of the oven the samples
 188 where left to cool to room temperature on a flat and clean surface during 1h.

189 3.2-Film thickness measurements

190 Film thickness was determined from the same polymer-coated black drawdown
 191 cardboards (DCBs) used for gloss testing by means of an Etalon Microrapid 226 (Brown



& Sharpe, Sweden). The actual polymer FT
 was determined by subtracting a blank
 194 value (corresponding to the DCB) to the total thickness measured. A linear relationship
 195 between wet and dried FTs, would be expected, indicating proper drying and uniform
 196 film deposition. This was already implied in Eq.6 which also predicted higher dried FTs
 197 for solid-rich liquid coatings (see Eq. 27 for the case where $\varphi_0 = \varphi_f$, $\rho_0 = \rho_f$ and
 198 completely dried film) .

$$\begin{aligned} \delta_f &= \Delta\delta_D - \delta_s \\ \delta_f &= \sqrt[3]{w_0} \cdot \delta_0 \end{aligned} \quad (27)$$

199

200 The value of δ_s is obtained for each coating extension test as the average value of 10
 201 random measurements alongside the whole available extension surface.

202 Special care was taken in not damaging the film extension as gloss measurements where
 203 performed before FT measurements. Absence of film damage was inspected both
 204 visually (by two of the authors) and by means of a digital microscope (Swift digital M10T-
 205 BTW1, China).

206 3.3-Gloss measurements

207 The gloss of each sample was randomly recorded at least 10 times with a glossmeter
208 (REFO 3, HACH, Manchester-United Kingdom) according to UNE-EN-ISO 2813:1999. The
209 measurements were performed varying orientation clockwise and only after the
210 samples had been properly cooled.

211 3.4-Data analysis ,model validation and model comparison

212 The studied coatings were analysed by means of the following metrics [68]:

- 213 • Residuals magnitude and distribution
- 214 • Parity charts in which calculated gloss values have been compared towards
215 experimental values.
- 216 • Adjusted correlation factor R_{adj}^2
- 217 • Sum of squared errors (SSE) after finding the model parameters by minimizing
218 it using Excel® Solver GRG nonlinear algorithm.

219 Additionally the models have been compared to a previous one. The empirical model
220 presented by Bruce [67] has been used before for relating reflectivity and FT in glossy
221 coatings. Eq. 28 shows a substantial modification of Bruce's model in which gloss has
222 substituted reflectivity assuming they can be taken as equals.

$$g = g_s + \frac{(g_{sat} - g_s)\delta^2}{\delta^2 + C_B} \quad (28)$$

223 In Eq.28 C_B , is a material-related constant .The main difference between both models
224 (Eq. 24 and Eq.28) is that the latter tends to a saturation value g_{sat} gloss whilst the
225 former tends to infinite gloss values. Since gloss cannot increase infinitively (as viscosity
226 can) it will only work for moderately thin layers. As expected, the maximum film
227 thickness (δ_{sat}) upon which the change in gloss will have physical meaning will be:

$$\delta_{sat} = \left(\frac{g_{sat}}{\rho t_1} \right)^{\frac{1}{t_2}} \quad (29)$$

228 And, in turn, the maximum allowable gloss attainable (g_{sat}) will be :

$$g_{sat} = g_s + J(\delta_{sat}) \rho \delta_{sat}^{t_2} \quad (30)$$

229 Eq. 29 and Eq.30 provide interesting tools for comparing and characterising coatings.

230 δ_{sat} value may also be of use for assessing the range of validity of non-finite gloss

231 mathematical models⁸. Namely:

$$\begin{aligned} g &= g_s + J(\delta) \rho \delta^{t_2} & 0 \leq \delta \leq \delta_{sat} \\ g &= g_{sat} & \delta \geq \delta_{sat} \end{aligned} \quad (31)$$

232 For each kind of coating the following steps and formulas will be used for parameter

233 estimation. Gloss has been expressed on a relative basis G_i (Eq.31) for the calculations

234 involving glossy coatings:

$$G_i = \frac{g_i - g_s}{g_s} \quad (32)$$

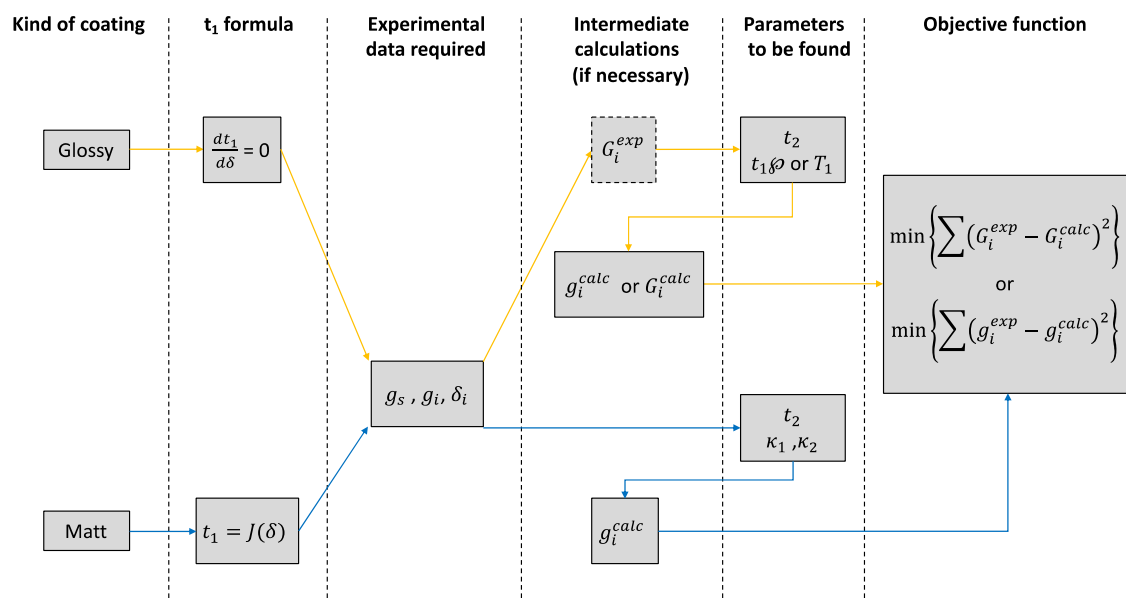
235

236

⁸ This piecewise mathematical formulation is a necessary consequence of using simplistic models.

237 4-Results

238 In order to validate the modelling approach presented in the previous sections several
 239 datasets have been used. Such datasets cover a wide range of both organic and
 240 inorganic substance, either with matting or glossy properties and even measured at
 241 different reference angles. The main idea behind the heterogeneity of the data was
 242 checking for the eventual limitations one might encounter when using Eq.26 for its
 243 description. Fig.4 summarizes for each kind of coating which parameters, measurements
 244 and procedures have been implemented.



245

246 **Fig4.** Flowchart for model parameter estimation

247 4.1-Glossy dataset

248 Four glossy inorganic coatings (Zinc oxide, zinc oxide + rubber, zinc sulphide and
 249 litophone⁹), two kinds of organic lacquers, one glossy PUD-base topcoat and three
 250 different-weaved silk fabrics have been investigated. Dataset 1 can be found in Table 1.

⁹ Litophone: A material obtained as a result of the coprecipitation of BaSO₄ and ZnS [73].

251 4.2-Matt dataset

252 Two PUD-based matting agents along with two purely inorganic silica coatings of varying
253 particle size and three PVC-TiO₂ films with increasing matting content have been tested.

254 Dataset 2 can be found in Table 2.

255

256

257

258

259

260

261

262

263

264

265

266

267

268

269

270

271

272

273

274

275

276

277

278

279

280
281
282

Table 1: Film-thickness vs gloss of different glossy coatings/materials (Dataset 1).

ID	Name	Data	Details and comments														
1	Lacquer_1 (Blank)	DFT (μm)	0	8	15	Source: [69] Multi-layered systems.											
		Gloss@60°	29	68	88												
2	Lacquer_2 (Hybrid)	DFT (μm)	0	7	13	The lacquer's substrate consists of SPCC steel disks with $g_s \approx 29 \text{ GU@60}^\circ$.											
		Gloss@60°	29	77	93												
3	Lit	DFT (μm)	0	9.76	14.6	17.1	29.3	45.3	53.7	Reflectance is here approximated as gloss value ($r \approx$ gloss measured towards no particular angle). The substrate is a perfectly matt black-asphalt paint.							
		r	0	40.8	58.2	62.7	79.5	89.5	91.2								
4	ZnO	DFT (μm)	0	7.32	10.9	17.1	23.2	30.5	36.6			47.6	Source: [65] Inorganic coatings.				
		r	0	28.4	35.2	53.9	60	72.7	75			80.2					
5	ZnORb	DFT (μm)	0	14.6	19.5	24.4	34.2	44.3	56.2			Reflectance is here approximated as gloss value ($r \approx$ gloss measured towards no particular angle). The substrate is a perfectly matt black-asphalt paint.					
		r	0	41.5	50.3	55.5	67.3	74.3	78.8								
6	ZnS	DFT (μm)	0	7.32	9.76	13.4	22	29.3	Source: [70] Silk weaved in various patterns.								
		r	0	48.73	56.8	67	81.3	87.4									
7	JpTSilk	DFT (μm)	164	245	255	Source: [70] Silk weaved in various patterns.											
		Gloss@45°	7.92	7.63	11.7												
8	ChTSilk	DFT (μm)	179	243	274	The gloss value represents the average value between the maximum and minimum gloss obtained by the authors so as to account for the birefringence of the samples.											
		Gloss@45°	5.83	6.66	10.42												
9	MoriSilk	DFT (μm)	179	243	274	Source: This work. Glossy PUD Topcoat.											
		Gloss@45°	6.23	8.62	12.51												
10	Glossy_1	DFT (μm)	0	9.9	21.3	38.1	49.1	60.4				71.7	149.7	Source: This work. Glossy PUD Topcoat.			
		Gloss@60°	63.33	78.98	84.24	88.39	89.69	91.65				92.32	94.19				

283 **Table 2:** Film-thickness vs gloss of different matting coatings (Dataset 2).

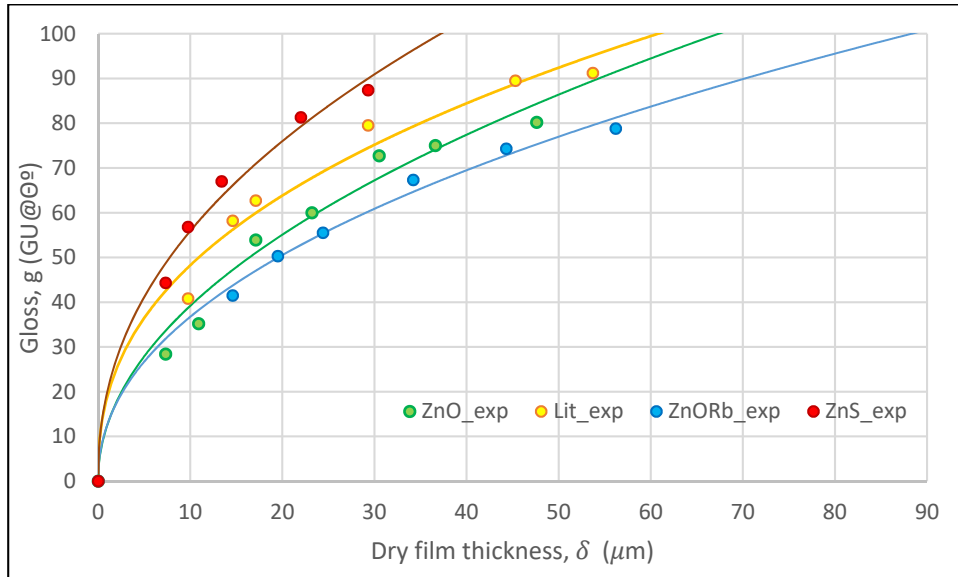
ID	Name	Data									Details and comments
11	Matt_1	DFT (μm)	0	7	11.3	16.2	18.1	26.9	27.9	30.8	Source: This work (PUD)
		Gloss@60°	63.6	4.89	1.74	1.88	1.7	2.13	2.02	2.36	
12	Matt_2	DFT (μm)	0	9.4	16.4	38.4	49.2	64.9	79.6	109.1	Matt_1: Hybrid matting agent. Matt_2: Traditional matting agent.
		Gloss@60°	63.09	2.4	0.68	0.46	0.64	1.02	1.02	1.1	
13	Matt_3	DFT (μm)	10	20	30	40	50	60	70	80	Source: [57] Samples with varying particle size. Matt_3: $d_p=5\mu\text{m}$; Matt_4: $d_p=3\mu\text{m}$. Matting agent concentration expressed as %w/w of SiO_2 ($x_m=3\%$).
		Gloss@60°	9.01	17.13	22.2	26.07	29.03	31.87	34.93	36.93	
14	Matt_4	DFT (μm)	10	20	30	40	50	60	70	80	Matting agent concentration expressed as %w/w of SiO_2 ($x_m=3\%$).
		Gloss@60°	10.02	20.13	28.13	32.87	38.27	42.33	45.4	48.33	
15	PVC_1	DFT (μm)	0	25.4	76.2	127	177.8	254	Source: [71] PVC-TiO ₂ films. Matting agent concentration expressed as %w/w of TiO ₂ . PVC_1 ($x_m=89\%$) PVC_2 ($x_m=57\%$) PVC_3 ($x_m=30\%$)		
		Gloss@75°	77.62	(*)	15.2	10.2	10.5	10.8			
16	PVC_2	DFT (μm)	0	25.4	76.2	127	177.8	254	Source: [71] PVC-TiO ₂ films. Matting agent concentration expressed as %w/w of TiO ₂ . PVC_1 ($x_m=89\%$) PVC_2 ($x_m=57\%$) PVC_3 ($x_m=30\%$)		
		Gloss@75°	77.62	39	16.6	17.2	12.2	13.8			
17	PVC_3	DFT (μm)	0	25.4	76.2	127	177.8	254	Source: [71] PVC-TiO ₂ films. Matting agent concentration expressed as %w/w of TiO ₂ . PVC_1 ($x_m=89\%$) PVC_2 ($x_m=57\%$) PVC_3 ($x_m=30\%$) (*) rejected data point from original source. The data point was clearly inconsistent showing poor substrate coverage or some issue with mixing.		
		Gloss@75°	77.62	43.4	21.6	19	15.2	19.4			

284
285
286
287
288
289

291 4.3-Model fitting

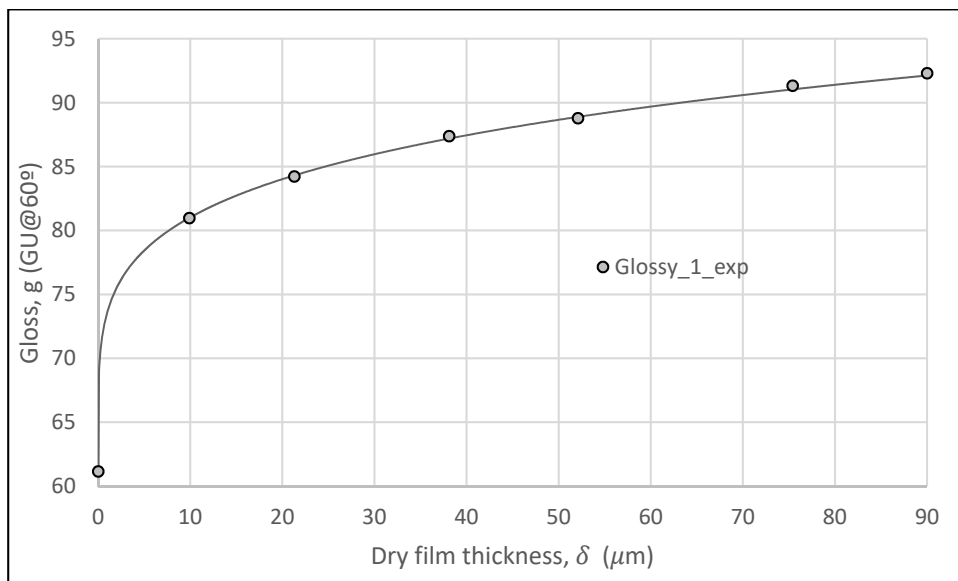
292 The data is plotted in Graphs 2 to 8, along with the corresponding mathematical models

293 forecasts . Fitting results are summarized in tables 2 and 3.



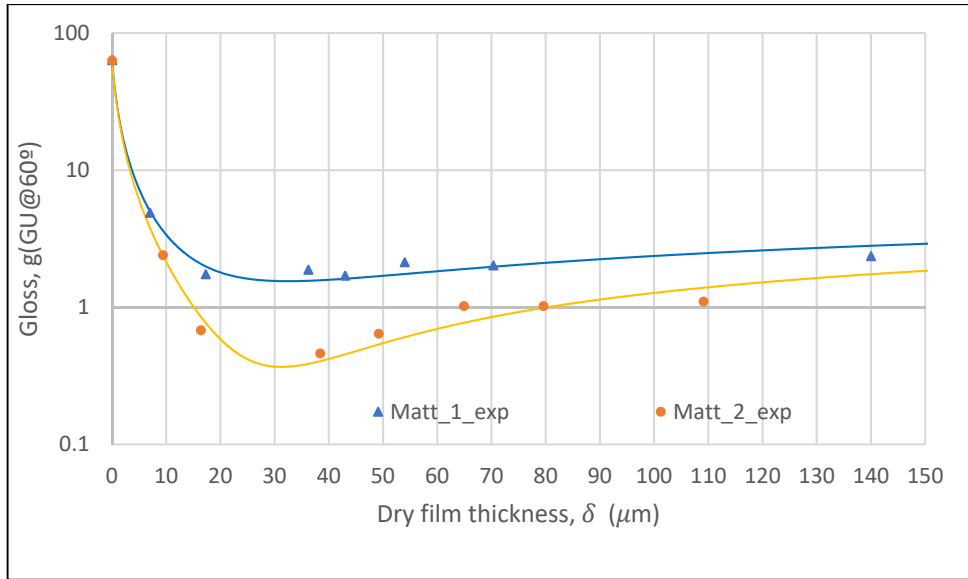
294
295
296

Graph 2: Film thickness effect on gloss for several inorganic glossy coatings.



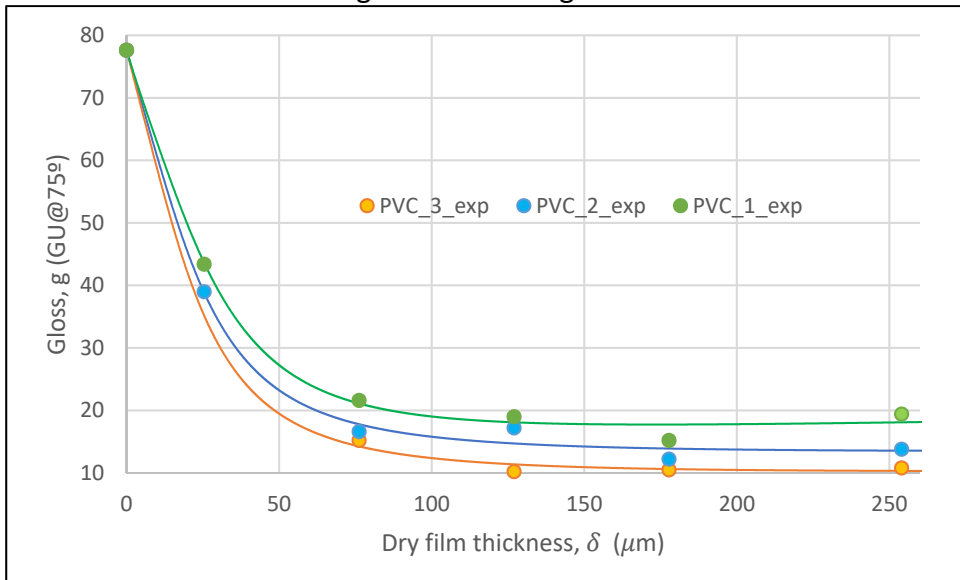
297
298
299
300

Graph 3: Film thickness effect on gloss for a PUD glossy topcoat.



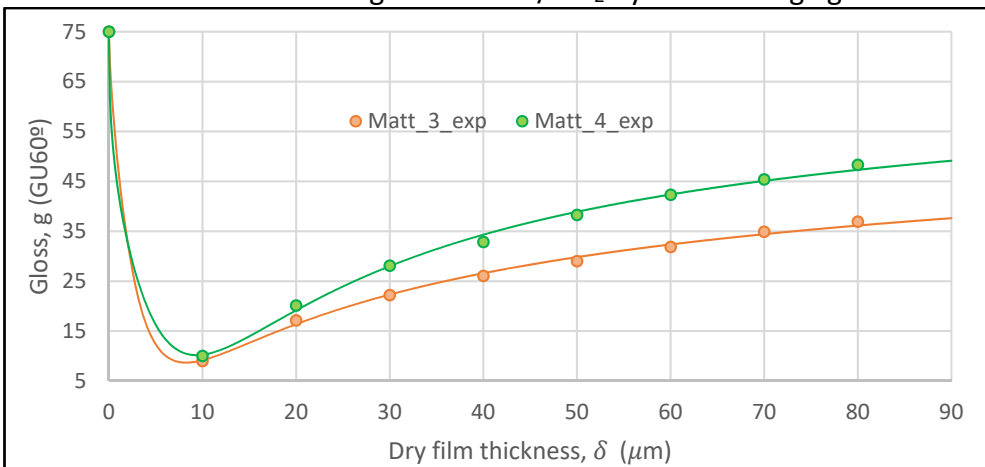
301
302

Graph 4: Film thickness effect on gloss for matting PUDs



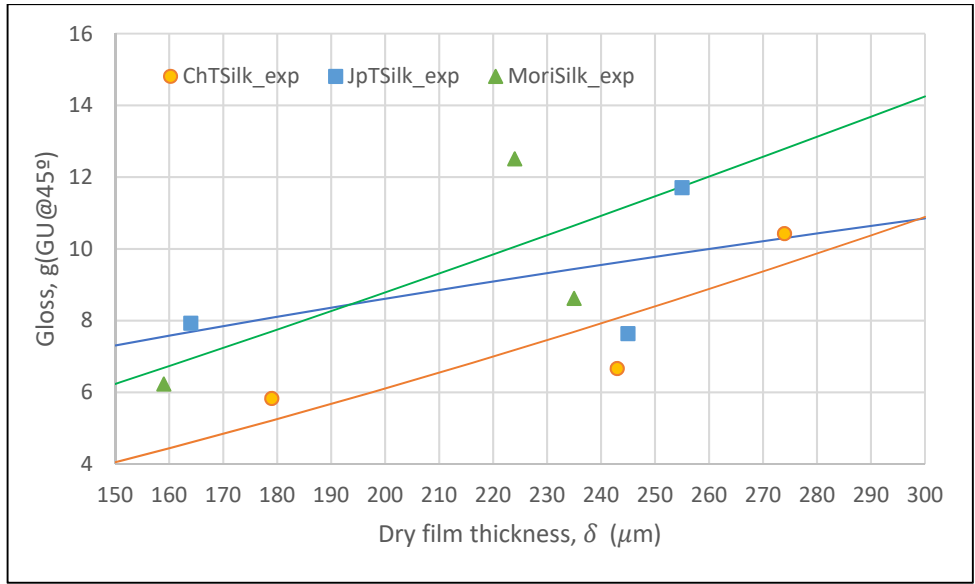
303
304
305

Graph 5: Film thickness effect on gloss for PVC/TiO₂ hybrid matting agents



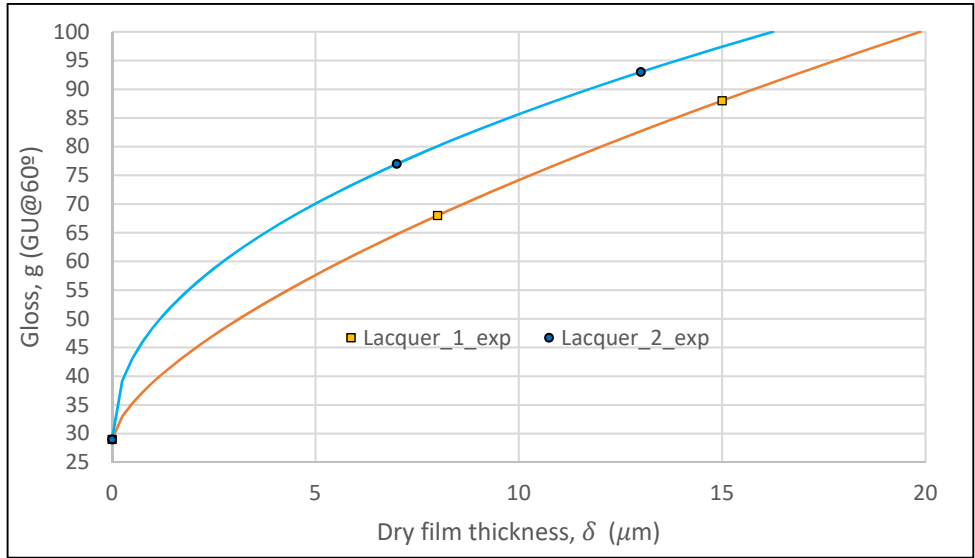
306
307
308

Graph 6: Film thickness effect on gloss for pure SiO₂ matting agents.



309
310
311

Graph 7: Film thickness effect on gloss for several weaved silks.



312

Graph 8: Film thickness effect on gloss for lacquers

313

314

315

316

317

318

319

320 **Table 2:** Metrics for glossy coatings

ID	Dataset	Fitted equations	SSE	R_{adj}^2	Parity equation	$\delta_{sat}^{calc\ 10}$ (μm)	$\delta_{sat}^{exp\ 11}$ (μm)
1	Lacquer_1	$g = 29 + 9.92 \cdot \delta^{0.66}$	10^{-7}	1.0000	$y = x$	19.72	-
2	Lacquer_2	$g = 29 + 19.43 \cdot \delta^{0.46}$	10^{-9}	1.0000	$y = x$	16.73	-
3	Lit	$g = 19.04 \cdot \delta^{0.45}$	101.4	0.9741	$y = 1.3654 + 0.9786x$	39.88	241
4	ZnO	$g = 11.2 \cdot \delta^{0.53}$	83.4	0.9791	$y = 2.8785 + 0.9575x$	62.22	190
5	ZnORb	$g = 11.69 \cdot \delta^{0.48}$	20.19	0.9899	$y = 0.3947 + 0.9930x$	87.51	152
6	ZnS	$g = 20.20 \cdot \delta^{0.44}$	43.6	0.9650	$y = 0.6958 + 0.9884x$	37.91	56.2
7	JpTSilk	$g = 0.42 \cdot \delta^{0.57}$	0.52	0.2749	$y = 6.5422 + 0.2796x$	-	-
8	ChTSilk	$g = 0.003 \cdot \delta^{1.43}$	0.86	0.7456	$y = 1.6565 + 0.7805x$	-	-
9	MoriSilk	$g = 0.016 \cdot \delta^{1.19}$	0.69	0.4860	$y = 4.8396 + 0.4705x$	-	-
10	Glossy_1	$g = 61.16 + 12.5 \cdot \delta^{0.2}$	0.26	0.9997	$y = 0.0093 + 0.9996x$	289.6	-

321

322 It can be seen that for weaved silks the values of t_1 is significantly small compared to the other materials. This is most likely due to the fact that
 323 the model does not accurately fit experimental data and consequently the model parameters lack physical meaning.

324

¹⁰ Assuming g_{sat} is 100% GU@ θ calculated by means of Eq.30.

¹¹ From [56].

325
326

Table 3: Metrics for matting coatings

ID	Dataset	Fitted equations	SSE	R_{adj}^2	Parity equation	δ^*	g_{min}
11	Matt_1	$g = 63.6 - 227.2 \cdot \tanh\left(\frac{0.31}{1 + \delta}\right) \cdot \delta^{0.970}$	0.54	0.9999	$y = 0.001 + 1.0000x$	32.5	1.55
12	Matt_2	$g = 63.1 - 192.7 \cdot \tanh\left(\frac{0.37}{1 + \delta}\right) \cdot \delta^{0.969}$	0.19	0.9999	$y = 0.001 + 0.9990x$	31.3	0.37
13	Matt_3	$g = 72 - 27.5 \cdot \tanh\left(\frac{6.47}{1 + \delta}\right) \cdot \delta^{0.656}$	0.25	0.9936	$y = 0.817 + 0.9811x$	8.3	8.67
14	Matt_4	$g = 72 - 32.1 \cdot \tanh\left(\frac{12.49}{1 + \delta}\right) \cdot \delta^{0.395}$	0.99	0.9974	$y = 0.3058 + 0.9919x$	9.4	10.18
15	PVC_1	$g = 77.62 - 1.96 \cdot \tanh\left(\frac{37.17}{1 + \delta}\right) \cdot \delta^{0.987}$	2.50	0.9968	$y = 0.003 + 0.9992x$	309.2	10.29
16	PVC_2	$g = 77.62 - 1.76 \cdot \tanh\left(\frac{39.57}{1 + \delta}\right) \cdot \delta^{0.985}$	10.5	0.9968	$y = 0.102 + 0.9964x$	323.5	13.51
17	PVC_3	$g = 77.62 - 1.69 \cdot \tanh\left(\frac{48.93}{1 + \delta}\right) \cdot \delta^{0.944}$	3.09	0.9939	$y = -0.668 + 1.014x$	177.0	17.4

327

328 Regarding what was presented in Eq. 13 several expressions were tested for modeling
329 $t_1 = J(\delta)$. Some of the main requirements for the mathematical model were to include
330 a hyperbolic trigonometric function and to predict a nonnegative minimum gloss value.
331 Eq. 21 shows a suitable expression for t_1 :

$$t_1 = \kappa_0 \tanh\left(\frac{\kappa_2}{\delta + 1}\right) \quad (32)$$

332 Where $\kappa_0 < 0$. When the aforementioned equation is plugged in Eq.14 the GFTR for
333 matting agents is finally devised:

$$g = g_s + \kappa_1 \delta^{t_2} \tanh\left(\frac{\kappa_2}{\delta+1}\right) \quad (33)$$

334 where $\kappa_0 \neq \kappa_1$. If $\frac{dg}{d\delta}$ is set to 0 it is found that $\delta^* = f(t_2, \kappa_2)$. For the sake of simplicity
335 only the results found using Eq.32 will be presented and further treatment of this section
336 will be developed in the discussion.

337

338 5-Discussion

339 5.1-General aspects

340 The goodness of fit of all mathematical models is high in regard of the different statistical
341 tests performed. High correlation coefficients values along with randomly distributed
342 residuals (calculated but not shown) , symmetric parity charts and low SSE asses the
343 usefulness of the equations presented in this contribution. The only systems which are
344 not well described by the mathematical models are those involving fabrics.

345 5.2-Matting agents of varying concentration

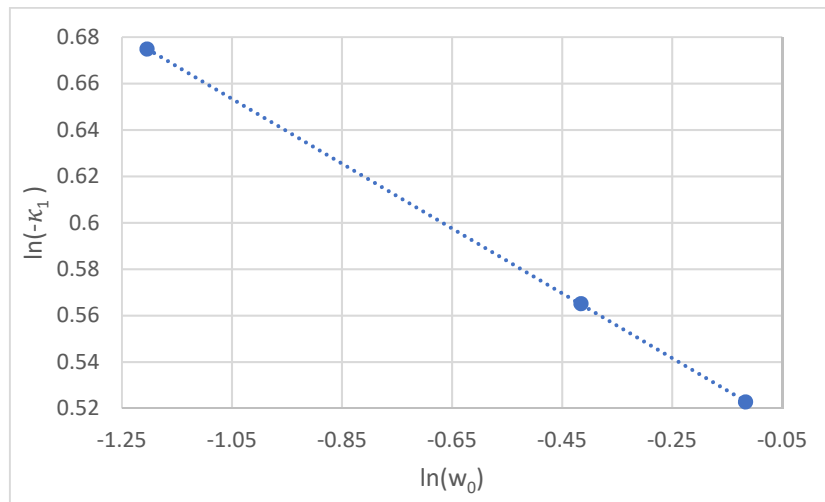
346 In agreement with the model derivation κ_1 is related to the matting agent concentration

$$\kappa_1 = \kappa_0 \left(\frac{\varphi_f w_{MA,f}}{\alpha \delta_0 \varphi_0 w_{MA,0}} \right)^{t_2} \quad (34)$$

347 if Eq.34 is linearized it can be shown that $\ln(-\kappa_1) \propto -t_2 \ln(w_{MA,0})$. Plotting the results

348 obtained for after fitting κ_1 for the PVC_1, 2 and 3 datasets confirms the model validity

349 in accounting for varying matting agent/matting polymer concentration:



350

351 **Fig. 6:** Functional dependence of model parameters with matting agent concentration.

352 5.3-Prediction of minimum gloss , δ^* and δ_{sat}

353 For a given matting agent its matting efficiency could be related to its minimum gloss. A

354 more efficient matting agent would require a smaller amount of coating so as to obtain

355 its minimum gloss. Despite this , experimental results do not provide conclusive results

356 in that regard.

357 The models undercalculate saturation film thickness values. This is probably due to the

358 fact that the original model does not account for that saturation behaviour.

359

360

361

362 5.4-Differences in t_2 value between matt and glossy coatings

363 After fitting the equations it became evident that whilst most of glossy coatings had a
364 power value between 0.5 and 0.7 as predicted by our modeling approach the matting
365 agents power value clustered around unity. This difference is most likely due to the fact
366 that the presence of matting agents (polymers/particles) rendered appreciable
367 alteration in film forming dynamics. Surface tension acts as a driving force for levelling
368 and plays an important part in reducing film area. According to this, for a coating with
369 hindered film formation, effective surface tension will be lower than expected. The film
370 forming driving force can be expressed as the difference between two Ohnesorge
371 numbers. Additionally, if $t_2 \approx 1$ it becomes evident that:

$$\Delta\sigma \propto \Delta\left(\delta^{\frac{1-t_2}{t_2}}\right) \rightarrow \Delta\sigma \approx 0 \quad (35)$$

372 Therefore, for matting agents (as expected), not so smooth films are obtained yielding
373 rough surfaces. The rheologic behaviour of the coatings will also play an important role
374 providing stresses are involved.

375 6-Conclusions and future work

376 Gloss and film thickness for several kinds of glossy and matt coatings have been
377 successfully correlated by means of easy-to-use models. The model derivation shows
378 consistency with important process variables such as matting agent concentration (as
379 seen in Fig.6). Glossy coatings can be represented by a power-like model where the
380 power value lies closer to 0.5-0.7 for Newtonian coatings. For non-Newtonian glossy
381 coatings the power value lies far from that interval showing strong deviations. Such
382 deviations were expectable given the fact that the new expression derived for $n=2$ was
383 based upon levelling time and momentum transference equation in which Newtonian

384 arguments where used. Interferences with surface tension levelling due to the presence
385 of matting agents have been also considered. The matting coatings follow a
386 hyperbolically modified power-law (loosely similar to Kubelka-Munk expressions) which
387 is able of predicting a minimum gloss value as it is found empirically.
388 Both presented models account for the substrate gloss (i.e. they meet the no coating
389 border condition) but since they are derived from a non-finite viscosity model they tend
390 to infinite gloss values instead of showing a saturation behaviour . Subsequently, a
391 piecewise function is required. δ_{sat} estimation is currently impossible as well. Other
392 surface defects such as micro-sagging or micro-bubbling cannot be accounted by the
393 mathematical model despite its relevance requiring specific mathematical treatment.
394 The case where a substantial degree of texture and optical isotropy (birefringence, etc.)
395 is found highlights another of the model's main limitations. For those cases, the model
396 fails in reproducing experimental data.

397 Future work concerning the present study should certainly deal with:

- 398 • A deeper exploration of the properties of the nondimensional equation $Oh =$
399 $f(Bo, Ca)$ and verifying its applicability in scale up /modeling. .
- 400 • A careful study of the influence of material properties such as density or viscosity
401 in model parameters such as saturation or minimum gloss and film thicknesses.

402

403 [References](#)

- 404 [1] J. Uribe-padilla, J. Salgado-valle, and M. Graells-Sobrè, "A novel contribution to
405 the modeling of the matting efficiency of aqueous polyurethane dispersions,"
406 *Prog. Org. Coatings*, 2017.
- 407 [2] L. A. Simpson, "Factors controlling gloss of paint films," *Prog. Org. Coatings*, vol.
408 6, no. 1, pp. 1–30, 1978.
- 409 [3] Z. W. Wicks, F. N. Jones, S. P. Pappas, and D. A. Wicks, *Organic coatings: science*
410 *and technology, Third edition*. 2007.

- 411 [4] A. A. Tracton, *Coatings Technology Handbook*. 2006.
- 412 [5] F. Martin, P. Muralt, M.-A. Dubois, and A. Pezous, "Thickness dependence of the
413 properties of highly *c*-axis textured AlN thin films," *J. Vac. Sci. Technol. A*
414 *Vacuum, Surfaces, Film.*, 2004.
- 415 [6] Y. Zhao, A. M. Nardes, and K. Zhu, "Solid-state mesostructured perovskite
416 CH₃NH₃PbI₃ solar cells: Charge transport, recombination, and diffusion
417 length," *J. Phys. Chem. Lett.*, 2014.
- 418 [7] B. Tlili, C. Nouveau, M. J. Walock, M. Nasri, and T. Ghrib, "Effect of layer
419 thickness on thermal properties of multilayer thin films produced by PVD,"
420 *Vacuum*, 2012.
- 421 [8] S. Mali, M. V. E. Grossmann, M. A. García, M. N. Martino, and N. E. Zaritzky,
422 "Mechanical and thermal properties of yam starch films," *Food Hydrocoll.*, 2005.
- 423 [9] G. Skordaris *et al.*, "Film thickness effect on mechanical properties and milling
424 performance of nano-structured multilayer PVD coated tools," *Surf. Coatings*
425 *Technol.*, 2016.
- 426 [10] K. D. Bouzakis *et al.*, "The effect of coating thickness, mechanical strength and
427 hardness properties on the milling performance of PVD coated cemented
428 carbides inserts," *Surf. Coatings Technol.*, 2004.
- 429 [11] J. H. Kuang and H. L. Chien, "The effect of film thickness on mechanical
430 properties of TiN thin films," *Adv. Sci. Lett.*, 2011.
- 431 [12] M. Buntinx *et al.*, "Evaluation of the thickness and oxygen transmission rate
432 before and after thermoforming mono- and multi-layer sheets into trays with
433 variable depth," *Polymers (Basel)*, 2014.
- 434 [13] C. Charton, N. Schiller, M. Fahland, A. Holländer, A. Wedel, and K. Noller,
435 "Development of high barrier films on flexible polymer substrates," in *Thin Solid*
436 *Films*, 2006.
- 437 [14] B. Bravin, D. Peressini, and A. Sensidoni, "Development and application of
438 polysaccharide-lipid edible coating to extend shelf-life of dry bakery products,"
439 *J. Food Eng.*, 2006.
- 440 [15] A. Kamel, D. Pascal, B. Isabelle, and L. Pierre, "Model predictive control of a
441 powder coating curing process: Application of the MPC@CB software," in
442 *Proceedings of the 26th Chinese Control Conference, CCC 2007*, 2007.
- 443 [16] R. Turton, "The application of modeling techniques to film-coating processes
444 Film coating," *Drug Development and Industrial Pharmacy*. 2010.
- 445 [17] D. He, Z. Wang, L. Yang, and Z. Mao, "Optimization control of the color-coating
446 production process for model uncertainty," *Comput. Intell. Neurosci.*, vol. 2016,
447 2016.
- 448 [18] T. M. Sullivan and S. Middleman, "Film thickness in blade coating of viscous and
449 viscoelastic liquids," *J. Nonnewton. Fluid Mech.*, vol. 21, no. 1, pp. 13–38, 1986.
- 450 [19] I. Iliopoulos and L. E. Scriven, "A blade-coating study using a finite-element
451 simulation," *Phys. Fluids*, 2005.
- 452 [20] R. W. Hewson and N. Kapur, "Effects of shear thinning on forward roll coating,"
453 *Chem. Eng. Res. Des.*, 2013.
- 454 [21] G. A. Zavallos, M. S. Carvalho, and M. Pasquali, "Forward roll coating flows of
455 viscoelastic liquids," *J. Nonnewton. Fluid Mech.*, 2005.
- 456 [22] E. V. A. N. M. Itsoulis and G. E. A. Thanasopoulos, "NUMERICAL SIMULATION OF
457 BLADE-OVER-ROLL COATING," *Comput. methods Mater. Sci.*, 2010.

- 458 [23] A. Javadi, H. S. Mehr, M. Sobani, and M. D. Soucek, "Cure-on-command
459 technology: A review of the current state of the art," *Prog. Org. Coatings*, 2016.
- 460 [24] M. Nabil and A. S. Rattner, "A Computational Study on the Effects of Surface
461 Tension and Prandtl Number on Laminar-Wavy Falling-Film Condensation," *J.*
462 *Heat Transfer*, 2017.
- 463 [25] D. Grosso, "How to exploit the full potential of the dip-coating process to better
464 control film formation," *J. Mater. Chem.*, 2011.
- 465 [26] X. Zhang, "Several fundamental researches on structural integrity of plasma-
466 sprayed coating-based systems," *Weld. World*, 2013.
- 467 [27] M. Javidi, M. A. Pope, and A. N. Hrymak, "Investigation on dip coating process
468 by mathematical modeling of non-Newtonian fluid coating on cylindrical
469 substrate," *Phys. Fluids*, 2016.
- 470 [28] L. Xu, X. Li, Y. Chen, and F. Xu, "Structural and optical properties of ZnO thin
471 films prepared by sol-gel method with different thickness," *Appl. Surf. Sci.*, 2011.
- 472 [29] J. P. Enríquez and X. Mathew, "Influence of the thickness on structural, optical
473 and electrical properties of chemical bath deposited CdS thin films," *Sol. Energy*
474 *Mater. Sol. Cells*, 2003.
- 475 [30] S. Y. Kim, "Simultaneous determination of refractive index, extinction
476 coefficient, and void distribution of titanium dioxide thin film by optical
477 methods.," *Appl. Opt.*, 1996.
- 478 [31] Q. Yong *et al.*, "Synthesis and surface analysis of self-matt coating based on
479 waterborne polyurethane resin and study on the matt mechanism," *Polym.*
480 *Bull.*, pp. 1–16, 2016.
- 481 [32] A. Goldschmidt and H.-J. Streitberger, "Basics of coating technology," 2007, p.
482 30.
- 483 [33] C. Francis, "Thickness of a Film Liquid Adhering to a Surface Slowly Withdrawn
484 from the Liquid," *NIST*, vol. 25, 1940.
- 485 [34] A. W. Crook, "The Lubrication of Rollers II. Film Thickness with Relation to
486 Viscosity and Speed," *Philos. Trans. R. Soc. A Math. Phys. Eng. Sci.*, vol. 254, no.
487 1040, pp. 223–236, 1961.
- 488 [35] B. Derjaguin, "On the Thickness of the Liquid Film Adhering to the Walls of a
489 Vessel after Emptying," *Prog. Surf. Sci.*, vol. 43, no. 1–4, pp. 134–137, 1993.
- 490 [36] L. Cisneros-Zevallos and J. M. Krochta, "Dependence of Coating Thickness on
491 Viscosity of Coating Solution Applied to Fruits and Vegetables by Dipping
492 Method," *Food Eng. Phys. Prop. Depend.*, vol. 68, no. 2, 2003.
- 493 [37] A. Lee, P.-T. Brun, J. Marthelot, G. Balestra, F. Gallaire, and P. M. Reis,
494 "Fabrication of slender elastic shells by the coating of curved surfaces," *Nat.*
495 *Commun.*, vol. 7, pp. 1–7, 2015.
- 496 [38] S. D. R. Wilson, "The drag-out problem in film coating theory," *J. Eng. Math.*, vol.
497 16, no. 3, pp. 209–221, 1982.
- 498 [39] L. Landau and B. Levich, "Dragging of a Liquid by a Moving Plate," *Acta*
499 *Physicochim. U.R.S.S.*, vol. 17, no. 1–2, pp. 42–54, 1942.
- 500 [40] H. N. Dixit and G. M. Homsy, "The elastocapillary Landau-Levich problem," *J.*
501 *Fluid Mech.*, vol. 735, pp. 1–28, 2013.
- 502 [41] R. R. Eley, "Applied Rheology in the Protective and Decorative Coatings
503 Industry," *Rheol. Rev.*, vol. 3, pp. 173–240, 2005.
- 504 [42] H. Zhai, "Effect of Film Thickness on the Rheological Behaviors of Asphalt

- 505 Binders," *Asphalt*, no. 001373, pp. 7–14, 2000.
- 506 [43] M. A. and K. K. Shin Kasahara , Hirota Saito , Makoto Hosotani, Noriko
507 Hatakeyama, "Relation between Viscosity and Film Thickness of Dental Luting
508 Cements," *Prosthodontics*, 2001.
- 509 [44] S. Wu, L. Pang, G. Liu, and J. Zhu, "Laboratory Study on Ultraviolet Radiation
510 Aging of Bitumen," *J. Mater. Civ. Eng.*, vol. 22, no. August, pp. 767–772, 2010.
- 511 [45] A. F. Routh, "Drying of thin colloidal films.," *Rep. Prog. Phys.*, vol. 76, no. 4, p.
512 046603, 2013.
- 513 [46] C. Petersen, C. Heldmann, and D. Johannsmann, "Internal stresses during film
514 formation of polymer latices," *Langmuir*, vol. 15, no. 11, pp. 7745–7751, 1999.
- 515 [47] T. Ismail, *Modeling in Transport Phenomena*, no. October. 2009.
- 516 [48] I. Ludwig, W. Schabel, P. Ferlin, J. C. Castaing, and M. Kind, "Drying, film
517 formation and open time of aqueous polymer dispersions," in *European Physical
518 Journal: Special Topics*, 2009.
- 519 [49] A. Tracton, *COATINGS TECHNOLOGY FUNDAMENTALS, TESTING, AND
520 PROCESSING TECHNIQUES*. 2007.
- 521 [50] R. Keunings and D. W. Bousfield, "Analysis of Surface Tension Driven Leveling in
522 Viscoelastic Films," *J. Non-Newtonian Fluid Mech. Elsevier Sci. Publ. B.V*, vol. 22,
523 pp. 219–233, 1987.
- 524 [51] H. S. Kheshgi and L. E. Scriven, "The evolution of disturbances in horizontal
525 films," *Chem. Eng. Sci.*, vol. 43, no. 4, pp. 793–801, 1988.
- 526 [52] L. E. Rodd, T. P. Scott, J. J. Cooper-White, and G. H. McKinley, "Capillary break-
527 up rheometry of low-viscosity elastic fluids," *Appl. Rheol.*, vol. 15, no. 1, pp. 12–
528 27, 2005.
- 529 [53] S. J. Jeon, "Mechanisms of Print Gloss Development with Controlled Coating
530 Structure," 2002.
- 531 [54] P.-G. de Gennes, F. Brochard-Wyart, and D. Quéré, *Capillarity and Wetting
532 Phenomena*. 2004.
- 533 [55] G. H. McKinley, "Dimensionless groups for understanding free surface flows of
534 complex fluids," *Soc. Rheol. Bull.*, vol. July, no. 05, p. 8, 2005.
- 535 [56] A.H.Pfund, "A relation between the Brightness and hiding power of white-paint
536 pigments," *Ind. Eng. Chem.*, 1930.
- 537 [57] J.Bieleman, *Additives for Coatings*, vol. 41, no. 1–3. 2001.
- 538 [58] G. P. Bierwagen, "Estimation of film thickness nonuniformity effects on coating
539 optical properties," *Color Res. Appl.*, vol. 17, no. 4, pp. 284–292, 1992.
- 540 [59] A. Goldschmidt and H.-J. Streitberger, *Basics of coating technology*. 2007.
- 541 [60] T. E. Fletcher, "A simple model to describe relationships between gloss
542 behaviour, matting agent concentration and the rheology of matted paints and
543 coatings," *Prog. Org. Coatings*, vol. 44, no. 1, pp. 25–36, 2002.
- 544 [61] T. J. Dougherty and I. M. Krieger, "Potential Around a Charged Colloidal Sphere,"
545 *J. Phys. Chem.*, vol. 63, no. 11, pp. 1869–1872, 1959.
- 546 [62] W. Wendlandt and H. Hecht, *Reflectance Spectroscopy*. 1966.
- 547 [63] C. Wiener, "Die Zerstreuung des Lichtes durch matte Oberflächen," *Ann. Phys.*,
548 vol. 283, no. 12, pp. 638–658, 1892.
- 549 [64] J. V. KOLESKE, *Paint and Coating Testing Manual: 15th edition of the Gardner-
550 Sward handbook*. 2012.
- 551 [65] L. Gamble and A. H. Pfund, "Experimental Determination of Brightness-Film

- 552 Thickness Curves of," *Ind. Eng. Chem.*, pp. 63–66, 1930.
- 553 [66] P. G. Judd DB, Harrison WN, Sweo BJ, Hickson EF, Eickhoff AJ, Shaw MB, "Optical
554 Specification of Light*scattering Materials," *J Res Nat Bur Stand*, vol. 19, pp.
555 287–317, 1937.
- 556 [67] H. D. Bruce, *A photometric method for measuring the hiding power of paints*,
557 vol. 20, no. no 306. 1926.
- 558 [68] G. E. P. Box, J. S. Hunter, and W. G. Hunter, "Statistics for Experimenters," in
559 *Statistics for Experimenters: Design, Innovation and Discovery*, 2005.
- 560 [69] R. Lu and T. Miyakoshi, *Lacquer Chemistry and Applications*. 2015.
- 561 [70] H. Kato, T. Hata, and T. Takahashi, "Characteristics of wild silk fibers and
562 processing technology for their use," *Japan Agric. Res. Q.*, vol. 31, no. 4, pp.
563 287–294, 1997.
- 564 [71] G. H. Al-Ghamdi, E. D. Sudol, V. L. Dimonie, and M. S. El-Aasser, "High PVC film-
565 forming composite latex particles via miniemulsification, Part 1: Preparation," *J.*
566 *Appl. Polym. Sci.*, vol. 101, no. 6, pp. 4504–4516, 2006.
- 567 [72] D. B. Hall, P. Underhill, and J. M. Torkelson, "Spin coating of thin and ultrathin
568 polymer films," *Polym. Eng. Sci.*, 1998.
- 569 [73] H. G. Völz, "Pigments, Inorganic, 1. General," in *Ullmann's Encyclopedia of*
570 *Industrial Chemistry*, 2012, pp. 225–256.
- 571
- 572